

TECHNOLOGY

Microfluidic isolation of extracellular vesicles and validation through AFM and DNA amplification

Srinivas Bathini¹, Shanmugasundaram Pakkiriswami², Duraichelvan Raju¹, Simona Badilescu¹, Anirban Ghosh¹, Rodney J. Ouellette³, Muthukumaran Packirisamy^{1,*}

¹Optical Bio-Microsystems Laboratory, Department of Mechanical Engineering, Concordia University, Montreal, Canada;

²Department of Biochemistry and Molecular Biology, Dalhousie Medicine New Brunswick, Saint John, New Brunswick, Canada;

³Atlantic Cancer Research Institute, Moncton, New Brunswick, Canada

*Correspondence to: Muthukumaran Packirisamy, Email: pmuthu@alcor.concordia.ca, Tel: +514 8482424 ext 7973

Received: 07 August 2020 | Revised: 06 October 2020 | Accepted: 08 October 2020 | Published: 08 October 2020

© Copyright The Author(s). This is an open access article, published under the terms of the Creative Commons Attribution Non-Commercial License (<http://creativecommons.org/licenses/by-nc/4.0>). This license permits non-commercial use, distribution and reproduction of this article, provided the original work is appropriately acknowledged, with correct citation details.

ABSTRACT

Extracellular vesicles (EVs) or exosomes are nano-sized particles containing lipids, proteins, mRNAs, and microRNAs from their origin cells, thus playing a critical role in cell-to-cell communication. The currently existing detection methods are expensive, time-consuming and lack in yield and purity. Here, we present a simple microfluidics-based method to capture EVs by a novel affinity-based approach, using, instead of antibodies, a synthetic polypeptide, Vn96, that binds to the heat shock proteins (HSPs) present on the surface of EVs/exosomes. The captured EVs are detected by using the high sensitivity of the Localized Surface Plasmon Resonance (LSPR) property of gold nano-islands to any changes in their local environment. The microfluidic devices developed for the isolation of exosomes, contain multiple channels and a collection chamber to capture EVs. The capture and detection ability of the device is validated by AFM measurements of isolated EVs from the device and the measurement of gene copy number using droplet digital PCR (ddPCR). The results indicate that the developed device can capture and isolate the EVs from a very low sample volume, in less than 30 minutes, without affecting their size and shape, a major advantage compared to existing methods. Thus, the device can be considered as a prospective point of care apparatus for diagnostics in a clinical setting.

Keywords: Lab-on a chip, early diagnosis of cancer, microfluidics, ddPCR

INTRODUCTION

Cancer has a significant impact on societies across the world, being among the leading causes of mortality. Based on a statistical analysis, it is estimated that 1.73 million new cases were diagnosed in United States in 2018, and the number of new cases per year is expected to rise to 15 million by 2020 (Ferlay et al, 2015).

Rapid and early diagnosis is required to control disease progression and treatment, providing a drive to develop new diagnostic tools, suitable for rapid point-of-care

(POC) applications. In the past two decades, Lab-on-a-chip (LoC) technology has drawn significant interest from the researchers and industries for biomedical applications. The advantages of LoC include high-throughput; low sample and reagent consumption; short assay time; and multiplexed detection (Rojalin et al, 2019; Su et al, 2019). The technology has shown potential to improve molecular biomarker detection by offering sensitive and wide-ranging measurements in a compact format.

Microfluidics-based platforms have been developed for isolation and quantification of biomolecules and more

complex entities that show potential for early cancer detection. Among these are membrane bounded nano-scale extracellular communication organelles, the extracellular vesicles (EVs), ranging in size from 30nm-1000nm, which are shed into the extracellular space by almost all cells (Zhang et al, 2019). They transport the identity of their mother cells, as they carry proteins and nuclei acids, and, therefore, are a potential source of biomarkers for the diagnosis of the parent tumor and its state of malignancy, and other pathological conditions such as inflammatory and neurodegenerative diseases.

Current commonly used protocols for isolation and quantification of EVs involve filtration, ultra-centrifugation steps, followed by characterization by methods such as Nanoparticle Tracking Analysis (NTA), Dynamic Light Scattering (DLS) and Atomic Force Microscopy (AFM). Thus, the current techniques are not only time-consuming, the recovery of EVs is also relatively low.

The sensitivity of the Localized Surface Plasmon Resonance (LSPR) property of silver and gold nanoparticles (AuNPs) to any change in their surrounding medium forms the basis for label-free bio-sensing applications (Lee et al, 2006; Willets et al, 2007; Chung et al, 2011). Binding biomolecules to AuNPs or nano-islands, immobilized on a substrate, results in a red-shift of the LSPR bands or/and an increase in the absorbance of the band. The optical properties of AuNPs in terms of size and shape have been thoroughly studied and optimized for sensing applications (Dykman et al, 2011; Yeh et al, 2012). LSPR sensors, based on plasmonic nanostructures, are now widely used to interrogate biomolecular interactions in real-time. Despite the increasing interest in the LSPR phenomenon and its applications, there are only a few reports on the integration of LSPR biosensing into microfluidic platforms - an emerging field of plasmofluidics (Huang et al, 2009; Ozhikandathil et al, 2012; Ozhikandathil et al, 2015; Unser et al, 2015; Wang and Fan, 2016).

For the capture, quantification, and characterization of EVs, several LSPR-based microfluidic approaches have been developed (Mao et al, 2007; Im et al, 2014; Im et al, 2015). These approaches are attractive for clinical applications because of the requirement of low amounts of sample and reagents, and shorter reaction times. From small volumes of serum and cell culture medium, using anti-CD63 capture antibody coated on the surface of micro channels serum vesicles were captured and from them RNA was extracted (Chen et al, 2010). A similar immune-affinity approach was used for the capture of exosomes by Kanwar et al (2014). The microfluidic platform, ExoChip, developed by in the authors' laboratory, enables the isolation and, at the same time, visualization and molecular profiling of the captured exosomes, including the isolation of total RNA, using an on-chip fluorescent assay. Further advancing of microfluidic technology for the detection and molecular profiling of exosomes was done by Im et al (2014) who designed an SPR-based nano-plasmonic exosomes sensor (nPLEX) for the quantitative analysis of exosomes. To improve the sensitivity and enable portable operation, these authors used periodic nanohole arrays, patterned in

a gold film, functionalized with antibodies for sensing the surface proteins of exosomes from ovarian cancer cell lines.

Recently, our group developed an LSPR method for the capture of EVs, which involved a small synthetic polypeptide called Vn96 (Ghosh et al, 2014) instead of antibodies, on a gold (Au) nano-island sensing platform that has a high affinity toward exosomes (Duraichelvan et al, 2016; Bathini et al, 2018). The method was first validated at a macro level, by using gold nano-islands on glass substrates and carrying out the sensing protocol in a discontinuous manner. At each step, the spectral shift of the Au LSPR was measured and the one corresponding to the binding of exosomes to the biotin-Vn96 was used for calibration purposes. In order to enhance the sensitivity of the detection and to accomplish the molecular profiling of the captured EVs, a novel microfluidic device was designed. In this paper, we report the design and fabrication of this microfluidic device, the isolation of EVs captured using Vn96 in the device, and the validation of the isolated EVs through droplet digital PCR gene amplification.

MATERIALS AND METHODS

This section describes the fabrication of three-dimensional (3D) gold nano-islands on a glass substrate by thermal convection method. The self-assembly of gold nanoparticles to form a 3D nanostructure is based on the flow of colloidal solution, induced by evaporation at the interface of the substrate and solution.

Materials

Gold (III) chloride trihydrate ($\text{HAuCl}_4 \cdot 3\text{H}_2\text{O}$) and sodium citrate were purchased from Sigma Aldrich. The Sylgard® 184 elastomer kit for the polydimethylsiloxane (PDMS) fabrication was purchased from Dow Corning. De-ionized (DI) water with a resistivity of 18M Ω , used in all the experiments was obtained by using the NANO pure ultrapure water system (Barnstead). 11-mercaptoundecanoic acid in ethanol (Nano Thinks Acid 11), N-(3-Dimethylaminopropyl)-N'-ethylcarbodiimide hydrochloride (EDC) and N-Hydroxysuccinimide (NHS), phosphate buffered saline (PBS) were obtained from Sigma Aldrich, Canada. PBS tablets were dissolved in DI water at 0.1M concentration at a pH of 7.2. Streptavidin was purchased from IBA GmbH, and biotin-PEG-Vn96 and EVs from MCF7-CCM were supplied by the Atlantic Cancer Research Institute (ACRI), Moncton, N.B., Canada.

Fabrication of gold nano-islands

Fabrication of gold nano-islands on glass substrates includes the synthesis of gold colloidal solution (AuNPs) and, subsequently, the deposition of Au multilayers onto glass substrates by using the thermal convection method. Spherical gold nanoparticles were prepared by reduction of Gold (III) Chloride trihydrate ($\text{HAuCl}_4 \cdot 3\text{H}_2\text{O}$) (chloroauric acid) by sodium citrate, following Turkevich's method. Briefly, 15mg of Gold (III) Chloride trihydrate ($\text{HAuCl}_4 \cdot 3\text{H}_2\text{O}$) are added to 95ml of DI water in a beaker and heated to the boiling point. Then, 5ml of sodium citrate solution (2%, w/v) was added to the boiling solution, reducing ions to nanoparticles. Then, the reduced gold nanoparticles are

deposited onto a glass substrate and the morphology was tuned to form gold nano-islands (Kimling et al, 2016).

Design, simulation, and fabrication of microfluidic device

Microfluidic channel architectures were designed and simulated in COMSOL Multiphysics 5.2. The architecture scheme shows an inlet and outlet connected with a microfluidic channel, containing a collection chamber. The designs were analyzed for the streamline contours of fluid flow in the channel. The architecture of the channel was designed in such a way that the fluid covers the entire region of the collection chamber where the absorption spectra corresponding to the molecular interactions will be measured. The channel was 500 μm wide with a depth of 150 μm . The EVs collection chamber in the device was designed with a diameter of 5mm and a thickness of approximately 150 μm and can hold a maximum of 3 μl of sample volume. The predicted streamline contours of the design are shown in Figure 1A.

The microfluidic device with the channel of 200 μm wide and 200 μm depth consists of an inlet and outlet connected to a collection chamber of 5mm diameter where the EVs captured by Vn96 were collected. A mold for this design was fabricated on a silicon wafer, using standard fabrication process with a negative photoresist.

The PDMS base (pre-polymer) and curing agent were mixed in the ratio of 10:1 by weight. The PDMS mixture

was placed in a vacuum desiccator and degassed to remove air bubbles. Then, to make the PDMS microfluidic channel, PDMS was casted onto a mold on a silicon wafer made with a standard fabrication process. Prior to PDMS casting, the mold was silanized by using 100 μl of trichlorosilane at 60 $^{\circ}\text{C}$ for 1hr on a hot plate, by covering it with a petri dish. Then, the mold was placed in a petri dish and the PDMS mixture was poured on the wafer to a thickness of \sim 2mm and baked at 60 $^{\circ}\text{C}$ for 10hr. On the wafer containing the microfluidic channel, the PDMS layer was then cut into individual samples of predefined size. To form a microfluidic device, a PDMS slice cut from the mold is bonded with the glass substrate containing the gold nano-islands, using plasma bonding. Figure 1B shows the schematic of the microfluidic device.

Microfluidic setup for spectral measurements

The microfluidic device was illuminated with a UV/visible light source through a 600 μm optical fiber. The transmitted light from the device was collected through another 600 μm optical fiber, which is connected to the Ocean Optics USB4000 spectrometer. This spectrometer was linked to a computer through Spectrasuite software to measure the absorption spectra at each stage of the biosensing protocol. This spectrometer was custom built, and the arrangement could be modified as needed. In this setup, the optical fibers were placed vertically in such a way that the microfluidic device was positioned in-between the optical fibers aligned with the collection chamber. The light from the optical fiber

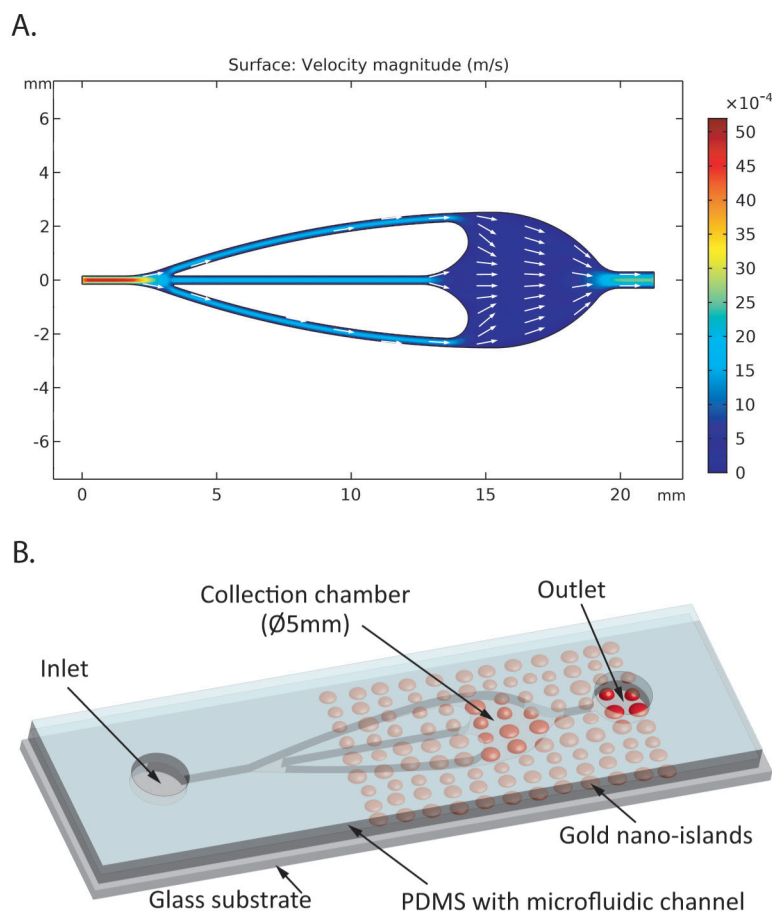


Figure 1. Predicted streamline contours in the designed microfluidic channels. **A.** streamline contours showing the magnitude of fluid velocity in the microfluidic channels, **B.** Schematic of the fabricated microfluidic device.

was shined on the device through a collimator to cover the entire area of the collection chamber. Then, the transmitted light was collected through another collimator, connected to the optical fiber that leads to the spectrometer. An attenuator was used in the setup to adjust the intensity of the light received from the device.

The biosensing protocol used to capture the EVs, an affinity-based approach developed in our laboratory, was published recently (Bathini et al, 2018). The EVs from the MCF7-CCM were used for microfluidic isolation and their size distribution was measured by NTA using NanoSight LM20 Nanoparticle Analysis System. The CCM was diluted by 100x for the measurement purposes and the size was around 100nm as shown in Figure 2. The schematic of the biosensing protocol and the schematic of the experimental setup including the Ocean Optics spectrometer, showing the flow of compounds using a syringe pump involved in the detection through the microfluidic device is shown in Figure 3A,3B.

Elution and characterization of EVs

The microfluidic devices were washed with PBS at a flow rate of 10 μ l/min to remove any unbound EVs from the collection chamber and the channel. Proteinase K (PK), which is a robust protein/peptide digesting enzyme, was prepared using PBS with a concentration of 20 μ g/ml and 12 μ l of proteinase K was used to elute EVs from the chip. PK was infused into the device to digest the protein/peptides bridging gold nano-islands and EVs so that the liquid flown out of the device will contain the EVs captured on the sensing platform. Proteinase K was flown to fill the entire channel and collection chamber and then the device was incubated at 37°C for 1hr. After incubation, ~15 μ l of PK was eluted from the device, called

eluent. The eluent, containing EVs, was characterized by AFM, and by gene copy number estimation amplification using ddPCR.

The size of the EVs from the eluent measured using a Park Systems XE-100 atomic force microscope by scanning in a non-contact mode, equipped with a silicon cantilever (f \sim 300 kHz, Park Systems). Topographic and phase images were recorded simultaneously at a scan rate of 1Hz and then processed using the Park Systems XE1 software.

The ddPCR analysis has been recently developed as an accurate way for absolute quantification of nucleic acids present in a very few numbers in the target samples. It has been used for absolute copy number quantitation and was shown to be more reliable than other digital PCR methods or any other conventional copy number determination methods. A droplet digital PCR was performed according to the manufacturer's instructions using the QX200™ Droplet Digital™ PCR System (Bio-Rad Laboratories) to determine the number of copies of RNaseP gene present in the EV samples that were eluted from the microfluidic chips. For the ddPCR reactions 2 μ l of collected eluent from the chips was used as template. The ddPCR reaction mixture consists of 10 μ l of Taqman probe assay (no dUTP) (Bio-Rad Laboratories) for a gene amplification in a total volume to 20 μ l reaction mix. Then, this 20 μ l volume of mixture was further mixed with 70 μ l of droplet generation oil and loaded onto a disposable plastic cartridge, covered with a specific gasket and placed in the droplet generator. For control, the eluent was replaced with PBS buffer. After droplet generation, samples were transferred to a 96-well PCR plate and, then, sealed, using the PX1 PCR plate sealer. Then, the PCR amplification was carried out in C1000 Touch™ Thermal Cycler (Bio-Rad laboratories) as

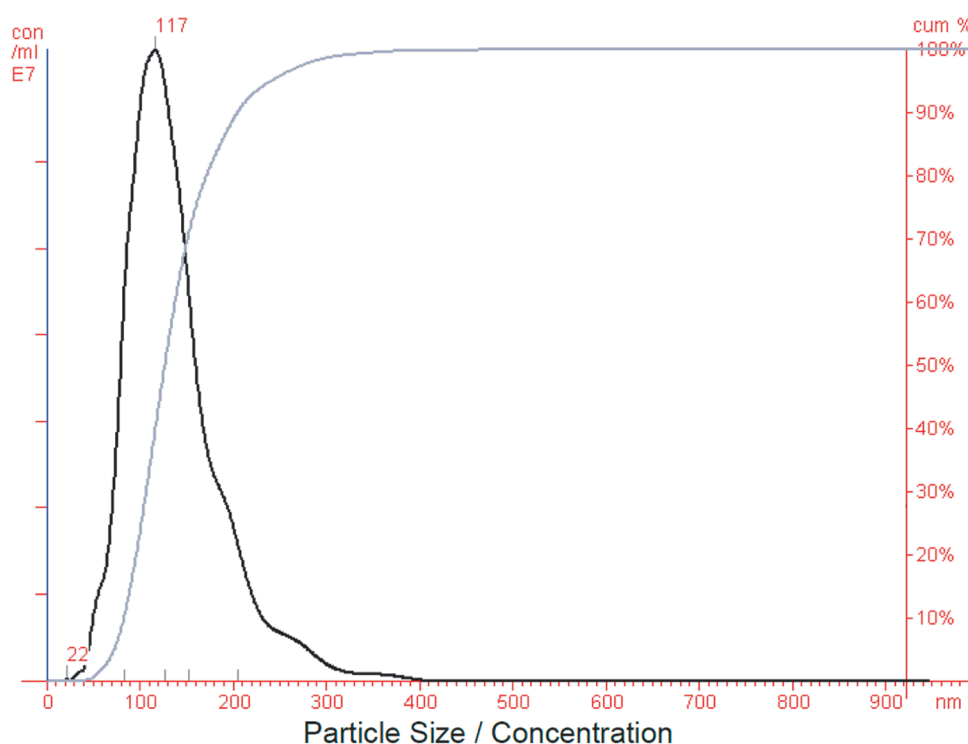


Figure 2. Representative figure that displays the size distribution of 100x diluted MCF7 CCM measured by NTA (NanoSight LM20 Nanoparticle Analysis System) with identical settings. The measurements were done in triplicate and the mean was calculated.

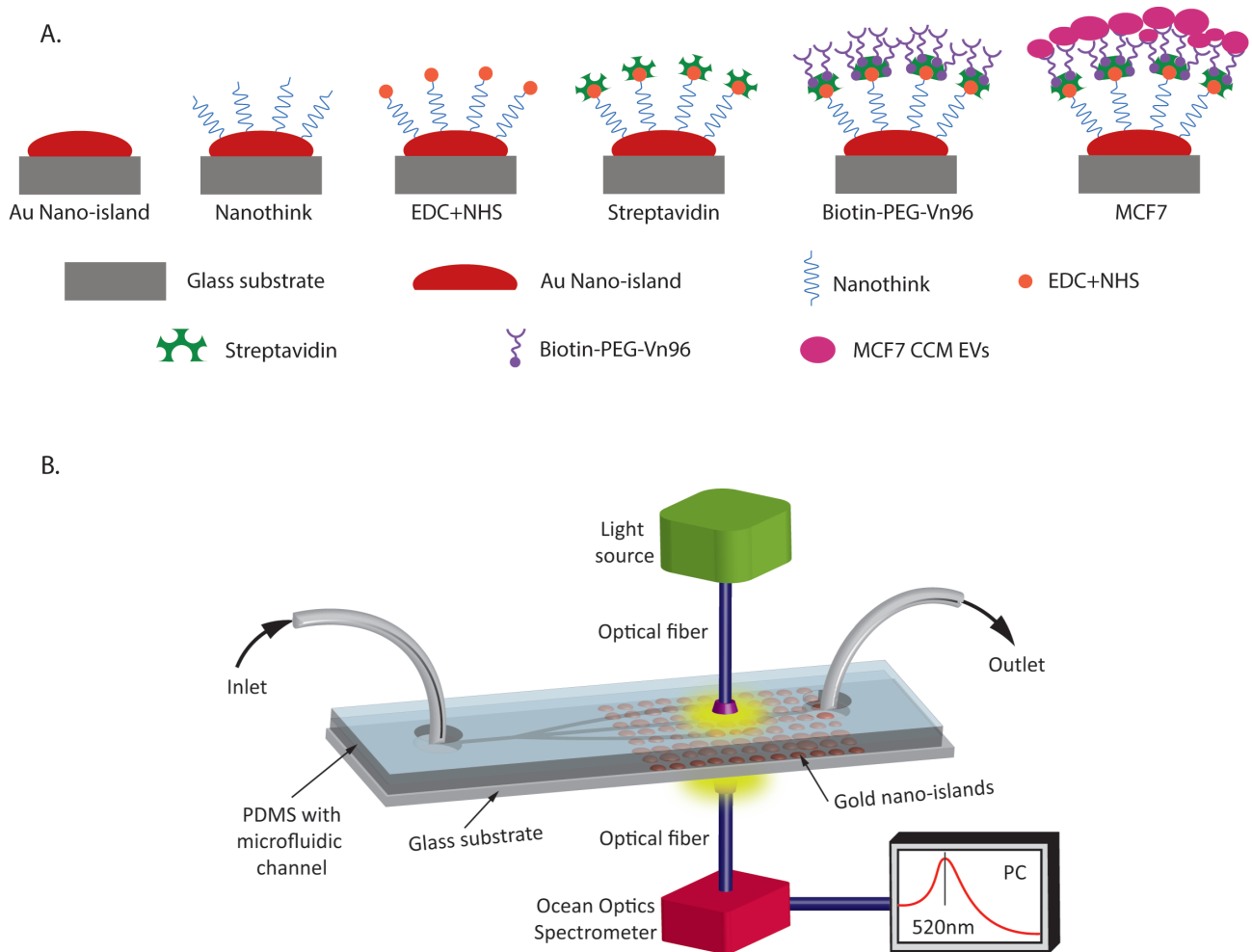


Figure 3. Microfluidic setup for the measurement of LSPR spectra. **A.** Schematic of the biosensing protocol used for the capture and isolation of EVs using Vn96 peptide. **B.** Schematic of microfluidic device used in an Ocean Optics spectrometer setup for the detection of isolated EVs using LSPR.

per the protocol provided by the manufacturer. After PCR amplification, the plate was shifted to the QX200™ Droplet Reader (Bio-Rad Laboratories), and the droplets from each well were automatically read for fluorescent signal detection. The Quanta Soft™ analysis software (Bio-Rad Laboratories) was used to analyze the data and quantify the copy numbers. A threshold signal value was set based on the resolution of positive and negative droplets to eliminate background noise.

RESULTS AND DISCUSSION

The absorption spectra were measured at each stage of the biosensing protocol using the Ocean Optics USB4000 spectrometer. As per the biosensing protocol, the volume, and concentrations of all the entities remain the same, except the concentration of MCF7 EVs. The LSPR shift corresponds to the molecular interactions, *i.e.* it quantitatively represents the number of EVs captured by the Vn96 in the microfluidic device. The LSPR shift ($\Delta\lambda$) has been measured at each stage of the protocol and the shift corresponding to various concentrations of extracellular vesicles is plotted in Figure 4. As expected, the shift is increasing as the concentration of EVs is increasing.

AFM-analysis of the eluted EVs

To validate the shifts in the LSPR spectral measurements of the microfluidic device, the eluent from the device was further analyzed by AFM. The samples were diluted to 1:100 with de-ionized water and adsorbed onto freshly cleaved mica sheets to perform AFM scanning. The topographic and phase images and line profiles of the EVs and control eluent are shown in Figure 5. It is noticeable from the image and line profile of the MCF7-CCM EVs eluent that the spherical particles are in the height and width of around 15nm and 60-80nm, respectively (Figure 5A). This size is within the size range of EVs published in the literature (Sharma et al, 2010; Chernyshev et al, 2015). The control eluent did not show any spherical particles, but mostly irregular shapes of heights around 1-2 nm, without any phase contrast (Figure 5B). The morphology of isolated EVs can be seen as spherical in shape from the line profiles with a diameter of around 80nm while the control shows irregular shapes of around 2nm. The size of isolated EVs is almost in agreement with the size shown by the NTA measurements. Therefore, the AFM measurements confirm that the proposed microfluidic devices have successfully captured and isolated the EVs from the CCM, validating the shift in the LSPR spectral measurements.

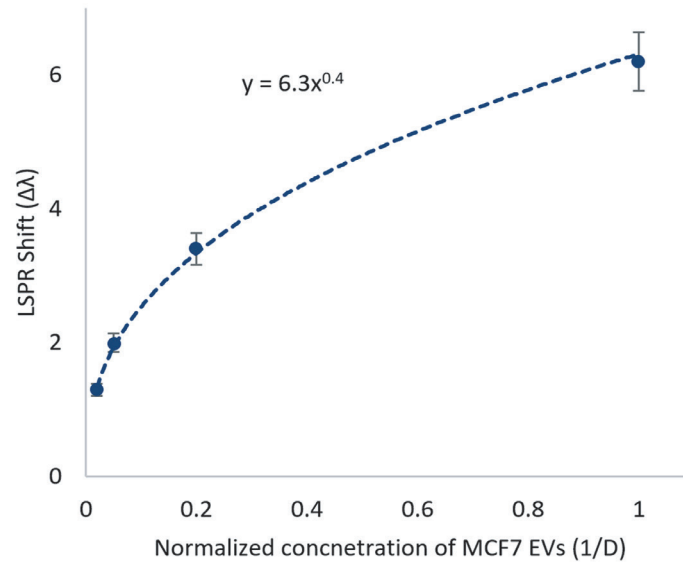


Figure 4. LSPR shift measured from the microfluidic device using the adopted biosensing protocol corresponding to various dilutions of MCF7 CCM EVs (Dilutions: 50x, 20x, 5x, and undiluted). Each data point can be tagged to identify the corresponding dilution of the sample (n=6).

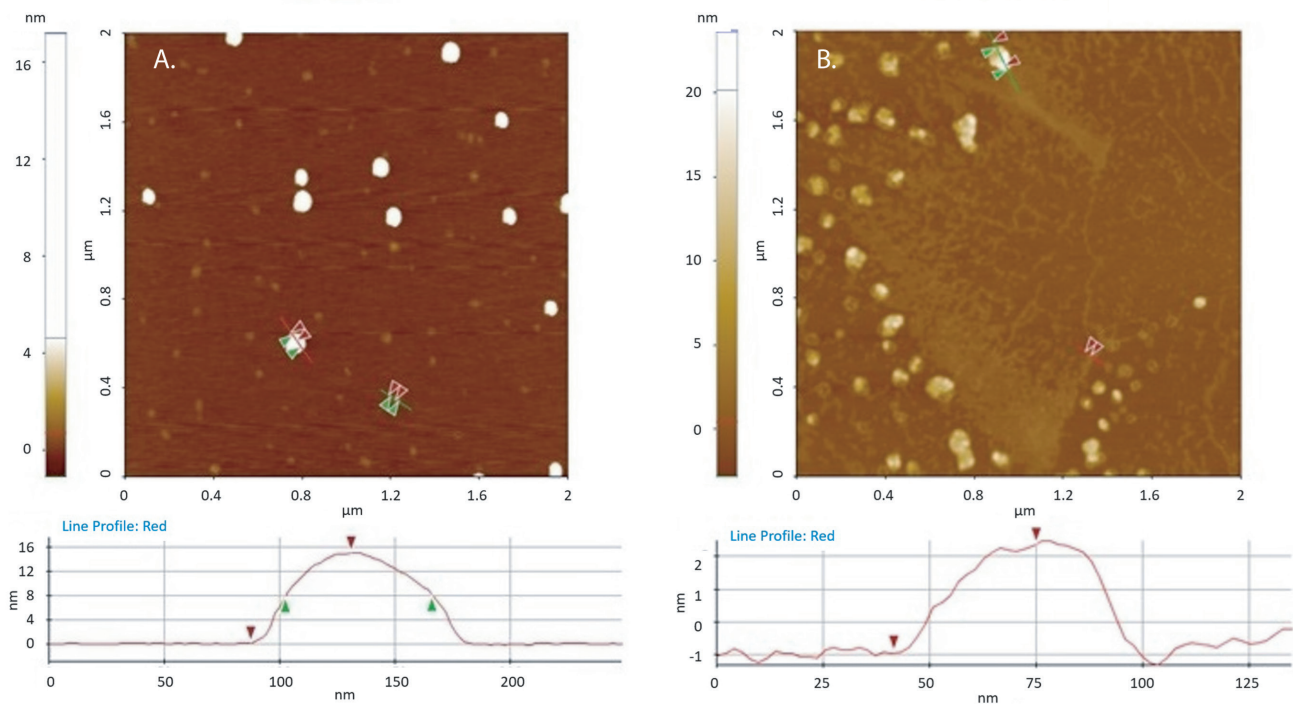


Figure 5. Morphology of isolated EVs by AFM phase images and line profiles. **A.** Phase image of the Vn96 peptide-precipitated (Proteinase K digested) EVs and its line profile. **B.** Phase image of the control sample, which is EV-free media that was used for culturing MCF7 cells and its line profile. A differential size distribution pattern is observed between EVs. The marked spots in the image are used to measure the width and thickness of two individual EVs.

RNase P gene copy number quantification by ddPCR

To further validate and investigate whether the gold-LSPR red shift observed is due to the high affinity binding of EVs to Vn96, droplet digital PCR (ddPCR) analysis was performed on the eluted fraction of EVs collected from the chips to quantitate the RNaseP DNA copy numbers as a reference gene. It has been shown that RNase P DNA sequence is present in the EVs and can be used as a reference gene in ddPCR reactions (Vagner et al, 2018). In this work, undiluted

and 5x times diluted MCF7-CCM was used to run through the chips to capture EVs. Initially, the concentration of undiluted MCF7-CCM EVs was measured by NTA and found to be 6×10^9 particles/ml and as per the designed protocol, only 100 μ l was used to run through the device. The number of RNase P gene copies from the eluent of undiluted and 5x diluted CCM infused microfluidic devices were found to be 3.66 and 1.08 copies/ μ l, respectively. As expected, the eluent collected from the microfluidic devices (MF-isolated

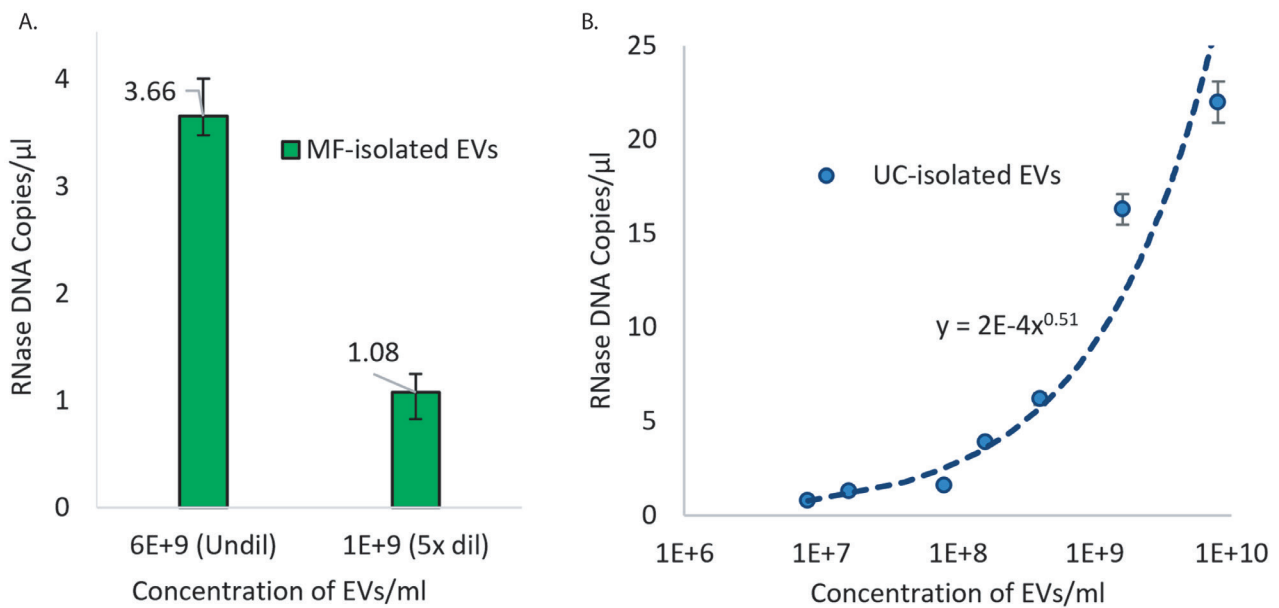


Figure 6. Quantification of isolated EVs by using droplet digital PCR (a) Number of gene copies amplified from microfluidic device eluent corresponding to undiluted and 5x diluted infused CCM (b) Number of RNase P gene copies amplified from various dilutions of UC-isolated EVs (n=3).

EVs) showed an appreciable number of RNaseP gene copies amplified by ddPCR reactions as shown in Figure 6A. This data validates that the red shift seen in the LSPR spectra is primarily due to the binding of EVs to the Vn96 in the devices.

In parallel, for comparison and as a positive control, EVs isolated through gold standard ultracentrifugation (UC-isolated EVs) at a concentration of 8×10^9 EVs/ml, was used for RNaseP gene amplification in ddPCR. Figure 6B shows the number of RNase P gene copies amplified with various dilutions of UC-isolated EVs. For negative controls, PBS buffer or EV-free CCM was used, and no amplification of RNase P DNA fragment was observed. By keeping the UC-isolated gene copies data as a reference, the 3.6 copies/ μ l determined through MF-isolated EVs corresponds to a concentration of approximately 1.6×10^8 EVs/ml. It means such a number of EVs should be captured in the collection chamber of the chip. On the other hand, in our recent work (Bathini et al, 2018), the physical modelling of Vn96-chip of the nano-island-EV interaction has shown that the collection chamber of 5mm diameter in a microfluidic device can accommodate up to a maximum of 5.3×10^8 EVs. As per the protocol, only 100 μ l of undiluted CCM, which corresponds to almost 6×10^8 particles, was infused into the microfluidic device. However, the chip was able to capture only $\sim 1.6 \times 10^8$ EVs by Vn96 present in the collection chamber. Similarly, with the 5x diluted CCM, only $\sim 1 \times 10^8$ EVs were captured out of 1.2×10^8 particles that were infused. It is interesting to note that capture capacity of Vn96 chip is better with diluted (5x) CCM compared to undiluted CCM. In 5x diluted CCM infused into the device, around 83% of the EVs infused were captured while in undiluted CCM, only 25% of the infused EVs got captured. This difference in the EVs captured and isolated, and the number of gene copies amplified from the eluent of microfluidic devices can be attributed to:

i) the efficiency of the Vn96 capture in the collection chamber and their specific binding with the HSP heavy EVs; ii) the loss of EVs that could have occurred during the Proteinase K mediated elution of EVs from the chip; iii) the presence of RNase P gene in the EVs as the this DNA fragment of the genome may not be present in all the EVs; iv) the number of gold nanoislands formed in the collection chamber; and v) aggregated EVs in highly concentrated CCM could prevent its binding with Vn96. Therefore, these data clearly show the capability of the microfluidic device for the isolation of EVs from a very low sample volume in less than 30 minutes.

CONCLUSIONS

Isolation and analysis of EVs are the cornerstones of any technique for EV-based diagnosis and therapeutic applications. In this study, we have demonstrated the capability of Vn96 enabled gold nanoisland-based microfluidic platform for capture and isolation of EVs originating from cancer cells and their DNA analysis through ddPCR reactions after eluting from the device. The gene amplification from the device and the AFM data showed that our microfluidic devices have the ability to bind, capture and isolate EVs from CCM, resulting in higher efficiency, and without affecting their size or shape. The major advantages of this label-free microfluidic technique include isolation of EVs from a very low sample volume in less than 30 minutes using a simple device, as compared with traditional techniques. In conclusion, the gold nanoisland-based microfluidic technique, with vn96-peptide functionalization, has a considerable potential in EV-based diagnosis in real-life clinical settings.

ACKNOWLEDGMENTS

The authors acknowledge the support of M Packirisamy from Natural Sciences and Engineering Research Council

of Canada (NSERC) and Concordia Research Chair and New Brunswick Innovation Fund (NBIF).

COMPETING INTERESTS

None declared.

LIST OF ABBREVIATIONS

EVs: Extracellular Vesicles
 HSP: Heat Shock Proteins
 LSPR: Localized Surface Plasmon Resonance
 AFM: Atomic Force Microscopy
 ddPCR: droplet digital Polymerase Chain Reaction
 LoC: Lab-on-a-Chip
 POC: Point-of-care
 NTA: Nanoparticle Tracking Analysis
 DLS: Dynamic Light Scattering
 AuNP: Gold Nanoparticle
 PDMS: Polydimethylsiloxane
 DI: De-ionized
 EDC: N-(3-Dimethylaminopropyl)-N'-ethylcarbodiimide hydrochloride
 NHS: N-Hydroxysuccinimide
 PBS: Phosphate buffered saline
 PEG – Polyethylene glycol
 CCM: Conditioned culture media
 PK: Proteinase K

REFERENCES

- Bathini S, Raju D, Badilescu S, et al. 2018. Nano-bio interactions of extracellular vesicles with gold nanoislands for early cancer diagnosis. *Research*, 3917986.
- Bathini S, Raju D, Badilescu S, Packirisamy M. 2018. Microfluidic Plasmonic Bio-Sensing of Exosomes by Using a Gold Nano-Island Platform. *Intl J of Biomed Biol Engg (WASET)*, 12, 226-229.
- Chen C, Skog J, Hsu CH, et al. 2010. Microfluidic isolation and transcriptome analysis of serum microvesicles. *Lab Chip*, 10, 505-511.
- Chernyshev VS, Rachamadugu R, Tseng YH, et al. 2015. Size and shape characterization of hydrated and desiccated exosomes. *Anal Bioanal Chem*, 407, 3285-3301.
- Chung T, Lee SY, Song EY, Chun H, Lee B. 2011. Plasmonic nanostructures for nano-scale bio-sensing. *Sensors*, 11, 10907-10929.
- Duraichelvan R, Srinivas B, Badilescu S, Ouellette RJ, Ghosh A, Packirisamy M. 2016. Exosomes Detection by a Label-free Localized Surface Plasmonic Resonance Method. *ECS Trans*, 75, 11-17.
- Dykman LA, Khlebtsov NG. 2011. Gold nanoparticles in biology and medicine: recent advances and prospects. *Acta Naturae*, 3, 34-55.
- Ferlay J, Soerjomataram I, Dikshit R, et al. 2015. Cancer incidence and mortality worldwide: Sources, methods and major patterns in GLOBOCAN 2012. *Int J Cancer*, 136, E359-E386
- Ghosh A, Davey M, Chute IC, et al. 2014. Rapid Isolation of Extracellular Vesicles from Cell Culture and Biological Fluids Using a Synthetic Peptide with Specific Affinity for Heat Shock Proteins. *PLoS ONE*, 9, e110443.
- Huang C, Bonroy K, Reeckmanns G, et al. 2009. Localized surface plasmon resonance integrated with microfluidic chip. *Biomed Microdevices*, 11, 893-901.
- Im H, Shao H, Park Y, et al. 2014. Label-free detection and molecular profiling of exosomes with a nano-plasmonic sensor. *Nature Biotechnol*, 32, 490-495.
- Im H, Shao H, Weissleder R, Castro CM, Lee H. 2015. Nano-plasmonic exosome diagnostics. *Expert Rev Mol Diagn*, 15, 725-733.
- Kanwar SS, Dunlay CJ, Simeone DM, Nagrath S. 2014. Microfluidic device (ExoChip) for on-chip isolation, quantification and characterization of circulating exosomes. *Lab Chip*, 14, 1891-1900.
- Kimling J, Maier M, Okenve B, Kotaidis V, Ballot H, Plech A. 2016. Turkevich method for gold nanoparticle synthesis revisited. *J Phys Chem B*, 110, 15700-15707.
- Lee KS, El-Sayed MA. 2006. Gold and silver nanoparticles in sensing and imaging: sensitivity of plasmon response to size, shape, and metal composition. *J Phys Chem B*, 110, 19220-19225.
- Mao X, Waldeisen JR, Juluri BK, Huang TJ. 2007. Hydrodynamically tunable optofluidic cylindrical microlens. *Lab Chip*, 7, 1303-1308.
- Ozhikandathil J, Badilescu S, Packirisamy M. 2012. Gold nanoisland structures integrated in a lab-on-a-chip for plasmonic detection of bovine growth hormone. *J Biomedical Optics*, 17, 077001.
- Ozhikandathil J, Badilescu S, Packirisamy M. 2015. Technical note: A portable on-chip assay system for absorbance and plasmonic detection of protein hormone in milk. *J Dairy Sci*, 98, 4384-4391.
- Rojalin T, Phong B, Koster HJ, Carney RP. 2019. Nanoplasmonic approaches for sensitive detection and molecular characterization of extracellular vesicles. *Front Chem*, 7, 1-24.
- Sharma S, Rasool HI, Palanisamy V, et al. 2010. Structural-Mechanical Characterization of Nanoparticle Exosomes in Human Saliva, Using Correlative AFM, FESEM, and Force Spectroscopy. *ACS Nano*, 4, 1921-1926.
- Su W, Li H, Chen W, Qin J. 2019. Microfluidic strategies for label-free exosomes isolation and analysis. *Trends in Anal Chem*, 118, 686-698.
- Unser S, Bruzas I, He J, Sagle L. 2015. Localized Surface Plasmon Resonance Biosensing: Current Challenges and Approaches. *Sensors (Basel)*, 15, 15684-15716.
- Vagner T, Spinelli C, Minciacchi VR, et al. 2018. Large extracellular vesicles carry most of the tumour DNA circulating in prostate cancer patient plasma. *J Extracell Vesicles*, 7, 1505403.
- Wang DS, Fan SK. 2016. Microfluidic Surface Plasmon Resonance Sensors: From Principles to Point-of-Care Applications. *Sensors (Basel)*, 16, 1175.
- Willems KA, Van Duyne RP. 2007. Localized Surface Plasmon Resonance Spectroscopy and Sensing. *Annu Rev Phys Chem*, 58, 267-297.
- Yeh YC, Creran B, Rotello VM. 2012. Gold nanoparticles: Preparation, properties, and applications in bionanotechnology. *Nanoscale*, 4, 1871-1880.
- Zhang Y, Liu Y, Liu H, Tang WH. 2019. Exosomes: biogenesis, biological function and clinical potential. *Cell Biosci*, 9, 19